

Optimize Gain Values of PI-Controller for Active Power Filter Using Mayfly Algorithm

Abdelmoezz Ahmed Eid*[‡], Ahmed Mohammed Attiya Soliman**, Mohammed A. Mehanna***

* Electrical Engineering Department, Al-Azhar University, Cairo, Egypt

** Electrical Engineering Department, Al-Azhar University, Cairo, Egypt

*** Electrical Engineering Department, Al-Azhar University, Cairo, Egypt

(engabdelmoezz@azhar.edu.eg, eng_ahmed1020@azhar.edu.eg, mehanna@azhar.edu.eg)

[‡] Abdelmoezz Ahmed Eid, Postal address: 11751, Tel: +201010688819, engabdelmoezz@azhar.edu.eg

Received: 07.09.2022 Accepted: 05.10.2022

Abstract- This article proposes an efficient optimization algorithm called Mayfly Optimization Algorithm (MOA) to configure a dc-link voltage with optimal PI-controller gains to enhance a three-phase three-wire shunt active power filter's dynamic performance (SAPF). The minimization of Total Harmonic Distribution (THD) is considered an objective function by optimizing the proportional and integral gain values of the PI-controller. The performance of the optimized controller is evaluated under variable load conditions. The effectiveness of the proposed algorithm is tested using the MATLAB/SIMULINK tool and compared with other optimization algorithms such as Particle Swarm Optimization (PSO), Artificial Hummingbird Algorithm (AHA), and Archimedes Optimization Algorithm (AOA). The simulation results prove the ability of MOA to get the optimal PI-Controller gains lead to optimizing the settling time, dc-link voltage overshoot, and steady-state error which attain enhancement of the SAPF controller performance and achieves THD in the drawing source current with minimum and acceptable values according to (IEEE-519) harmonics standard.

Keywords Power Quality, Total Harmonic Distortion, Shunt Active Power Filter, PI-Controller Tuning, Mayfly Optimization Algorithm.

1. Introduction

Excessive use of power electronics devices and non-linear loads in the Point of Common Coupling (PCC) generates harmonic currents that degrade electrical power quality (PQ) [1]. Because of the problems caused by the current harmonics in the distribution systems, such as loss, instability, noise, heating devices, etc.; therefore, it is desired to reduce their danger and reach the safe and permissible limit, where the Total Harmonic Distortion (THD) acceptable limits are provided by IEEE-519 standards [2].

Shunt Active Power Filter (SAPF) is an appealing method for current harmonics mitigation, reactive power compensation, and power factor correction. As shown in fig. 1, where the configuration of SAPF consists of two main parts: the active filter controller and the Voltage Source Inverter (VSI). The control unit is responsible for determining the instantaneous suitable firing signals, which are continuously

passed to the VSI which injects a controlled compensation current into the power system [3, 4]. The DC-link capacitor used in the VSI's front side is used to provide reactive power management to the grid [5]. VSI is necessary for connecting DC-side to the three-phase distributed power system. According to the firing signals, VSI injects a compensating current to limit distortion in the source current [6].

The VSI switching process is investigated using reference generating theories or control strategies. The SAPF control strategies can be applied in two stages: the first stage is extracting compensating signals from the distorted signals using the reference current generation theories, and the second stage is generating suitable firing signals to control the SAPF switching devices using the signal estimated reference methods [7]. In [8, 9] authors compared the different control strategies of SAPF.

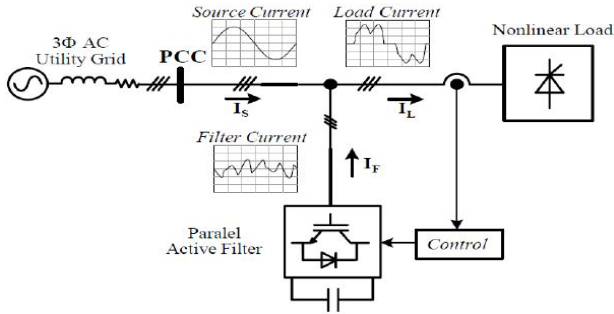


Fig. 1. The main components of SAPF and its integration at PCC [4].

Harmonic mitigation is handled by the PI-controller which is contained in reference current theory, where the K_p and K_i gain values of the PI-controller must be carefully optimized. The conventional method of tuning the PI-controller gains involves linear modelling and leads to the non-optimal tuning of gains [10, 11]. So, different metaheuristic optimization algorithms are used for PI-controller tuning. There are many control algorithms reduce current harmonics and add new possibilities to the converter [12]. For example, particle swarm optimization (PSO) [13-16], simulated annealing (SA), Atom Search Optimization (ASO) [17], and genetic algorithm (GA), [18]. Recently, new, and modified optimization algorithms are applied for the same purpose; therefore, this article aims to introduce robustness and efficient algorithms to achieve the target and reach the desired objective function compared with other algorithms.

In this paper, the reference current generation is based on instantaneous active and reactive power theory (PQ-theory). By the estimated reference currents, the required gating pulses are obtained using Hysteresis Band Current Controller (HBCC) method as shown in fig.2 [19]. The PI-controller for a dc-link voltage in PQ- theory needs the fine-tuning of its gain values, K_p and K_i . Further, the motivation of this article is based on a Mayfly Optimization Algorithm (MOA) which was proposed and tested against other previously and recently algorithms like (PSO), Artificial Hummingbird Algorithm (AHA), Archimedes Optimization Algorithm (AOA) to get the optimized PI – controller gain values and get the objective function with minimization of THD, and the performance of the optimized controller is evaluated under variable load conditions.

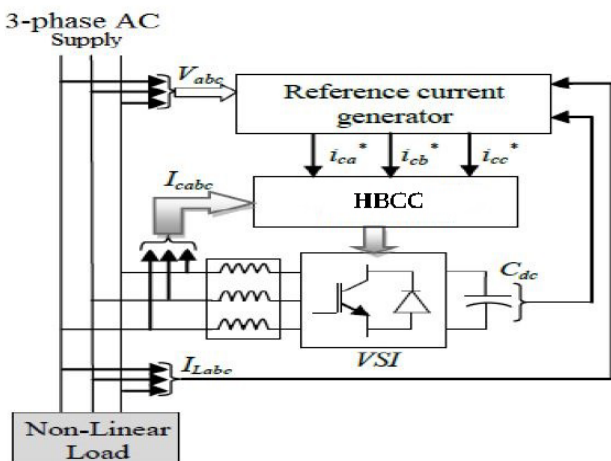


Fig. 2. Configuration of The SAPF Controller [19].

2. Proposed Controller of SAPF

2.1. The instantaneous active and reactive power theory (PQ-theory)

The constant instantaneous power control strategy based on PQ-theory has been designed for three-phase three-wire systems with sinusoidal and balanced source voltage. To implement this theory, the (a,b,c) three-phase values for source voltage and load current are sensed and transformed by Clarke transformation into (α,β) components which are the input signals for the instantaneous power calculation. the power losses component taken by a dc-link voltage based on the error signal which extracted from the reference and measured dc-link voltages values, then this error signal is introduced to a PI-controller to get (P_{loss}) . The (α, β) components with the active and reactive powers are handled too (α, β) current calculation to estimate the reference (α, β) current components which are inversed by inverse Clarke transformation to get the desired reference current signals as shown in Fig.3 [20- 24].

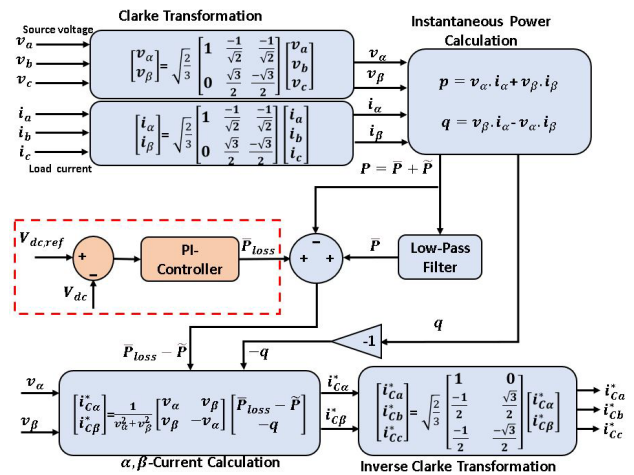


Fig. 3. Design of instantaneous active and reactive power theory.

2.2. Hysteresis Band Current Control (HBCC)

The Current signals obtained by the PQ-theory controller $i^*_{c a,b,c}$ and he actual injected currents $I_{c a,b,c}$ are given to the HBCC for generating the VSI necessary gating signals. Figure 4 shows the control phenomenon, where the output signals of the HBCC are the input pulses to the six switches (S1-6) of the VSI [25].

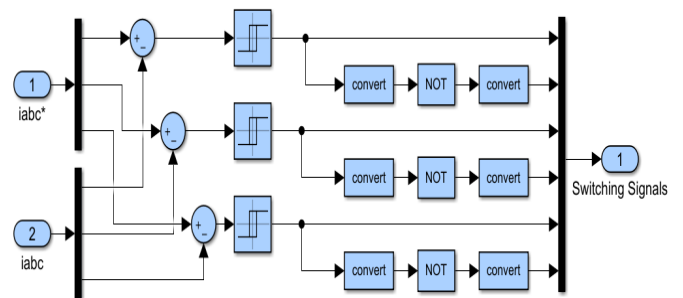


Fig. 4. HBCC and switching logic.

3. Mayfly Optimization Algorithm (MOA).

3.1. Mayfly Optimization Algorithm Definition

The MOA is an enhanced optimization algorithm. It combines the benefits of the PSO [14, 26], GA [27], and firefly algorithm (FA) [28] to provide a strong hybrid algorithm framework. The crossover technique and local search are employed based on the mayfly's social behaviors. By Assumption, after hatching the mayfly always will be an adult, and the strongest mayfly will survive. Each mayfly's location in the search space symbolizes a possible solution [29].

3.2. The MOA Principal Operation

The performance of the proposed solution which is represented by the n-dimensional vector $x = (x_1, x_2, \dots, x_n)$, which is made up of two swarms of mayflies, females, and males, is assessed using the pre-set objective function $f(x)$. The change in the mayfly's position is represented by a speed vector $v = (v_1, v_2, \dots, v_d)$. Each mayfly's flight path is the result of a dynamic interplay between their personal and communal flying experiences. The mayfly will specifically alter its course each time to obtain its personal best location, which is the best location attained by every mayfly in the swarm [30].

3.3. The Flow Chart of MOA

The steps of implementation of the MOA are clearly described by the flow chart shown in fig. 5, Where g_{best} is the global optimal solution, and p_{best} is the optimal location or position that mayfly has never been reached [31].

3.4. The Pseudo code for MOA

➤ **Input:** objective function $f(x)$, male population size (M_1), female population size (M_2), visibility coefficient (β), initial velocity for male mayfly (v_m), initial velocity for female mayfly (v_n), maximum iteration (T), a_1 and a_2 are positive attraction factors, solution dimension (d), population size (L)

➤ **Output:** Optimal Solution (g_{best})

1. **begin**
2. **Evaluate** all solutions according to the objective function $f(x)$
3. **Find** the best value from all solutions (g_{best})
4. **while** $t \leq T$
5. **find** p_{best} , the best solution for each male mayfly
6. **for** $I = 1:M_2$
7. **for** $j = 1:d$
8. Adjust female velocity
9. Adjust female positions
10. **end for**
11. **end for**
12. **for** $I = 1:M_1$
13. **for** $j = 1:d$
14. Adjust male velocity
15. Adjust male positions
16. **end for**

17. **Update** p_{best}
18. **end for**
19. **Rank** male mayflies
20. **Rank** female mayflies
21. **Mate** the mayflies
22. **Evaluate** the offspring
23. **Separate** offspring to male and female randomly
24. **Replace** the worst solution with the best new one
25. **Update** p_{best} and g_{best}
26. **end while**
27. **end**

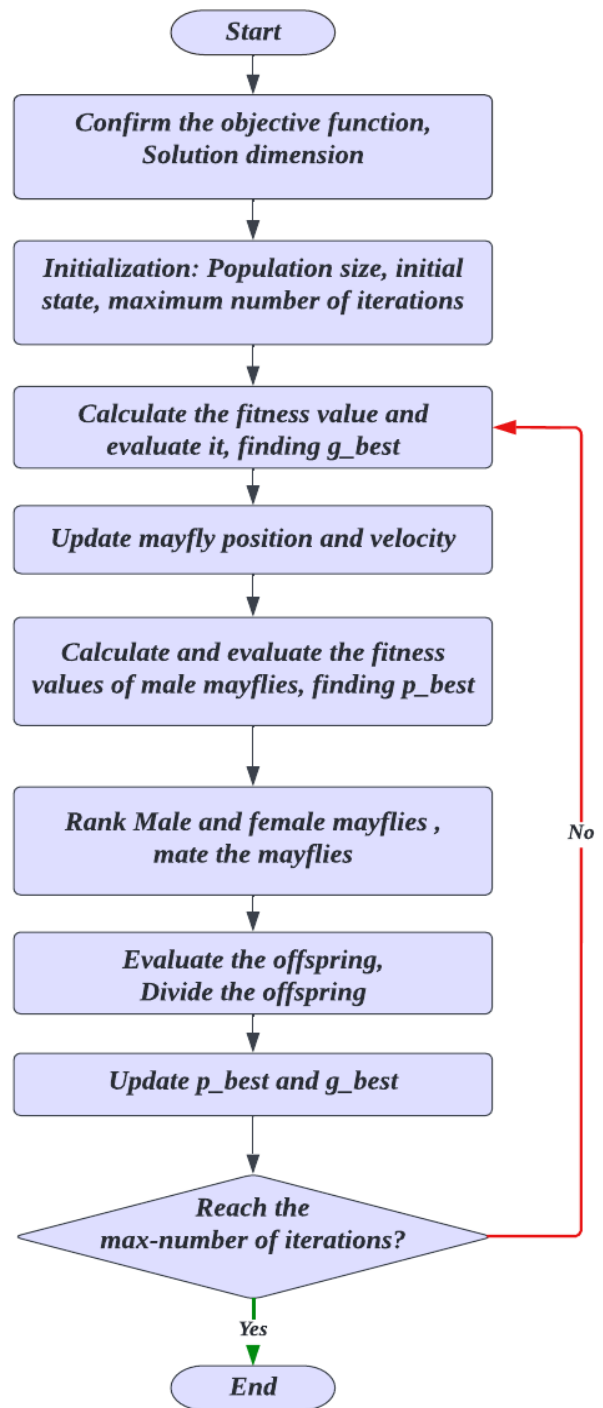


Fig. 5. The flow chart of the proposed algorithm (MOA)

4. The Problem Definition and Objective Function

The objective function of the Algorithms is to minimize the total Harmonic distortion of the source current THD_i. To do it, the PI-Controller gains K_p and the K_i are tuned and optimized by the proposed optimization algorithms as illustrated in fig. 6.

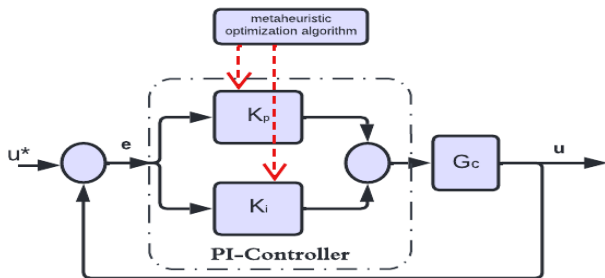


Fig. 6. Control System of PI-Controller by Optimization Algorithms

The THD_i is defined as the ratio of the RMS value of the total of all harmonic components up to a certain order to the RMS value of the fundamental component and can be expressed as in equation (1) [3, 7]. Where the gains are responding to the error and steady-state error respectively. The PI-controller transfer function is expressed as in equation (2), while the PI-controller output u(t) is given as in equation (3).

$$THD_i = \sqrt{\frac{\sum_{k=2}^{k_{max}} I_k^2}{I_1^2}} \tag{1}$$

$$G_c(s) = k_p + \frac{k_i}{s} \tag{2}$$

$$u(t) = e(t) + k_i \int_0^1 e(t) dt \tag{3}$$

where, e(t) is the error between the actual DC bus voltage (V_{dc}) and the reference DC bus voltage (V_{dc,ref}) [13].

5. Model Configuration

The proposed model configuration is illustrated in fig. 7, it contains a three-phase power grid connected to a three-phase un-controlled diode full bridge rectifier connected with an inductive load on the DC side which represent the non-linear load. At the PCC, SAPF with VSI design and capacitor on the DC link bus is integrated with the network.

The DC side capacitor reference voltage (V_{dc,ref}) is calculated as in equation 4, and the DC side capacitance (C_{dc}) value is calculated as in equation 5 [11].

$$V_{dc,ref} = \frac{2\sqrt{2}V_{LL}}{\sqrt{3}m} \tag{4}$$

$$\frac{1}{2} C_{dc} (V_{dc,ref}^2 - V_{dc}^2) = 3(V_s)(a)(t) \tag{5}$$

Where, (V_{LL}) is AC line voltage, (m) is the modulation index, (a) is the factor of over-loading chosen as 1.2, (V_s) is the source voltage, (I) is the phase current, and (t) is the recovery time of DC-bus voltage. The parameters of the model are listed in table 1.

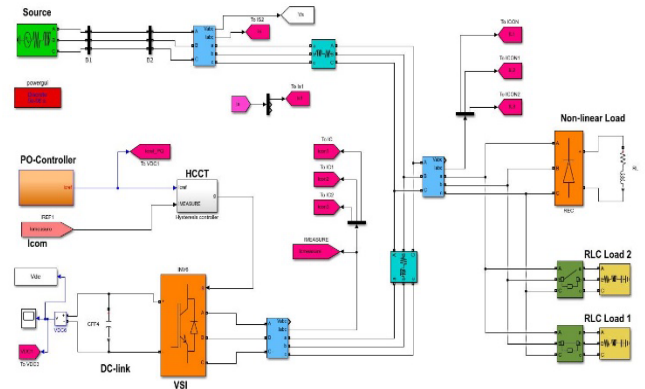


Fig. 7. MATLAB/Simulink model for the proposed configuration system

Table 1. Proposed System Parameters

System Parameters		Values
Supply Parameters	Voltage V _s	380 V
	Frequency f _s	50 Hz
	Source line resistor R _s	5 Ω
	Source line inductor L _s	2 mH
Non-Linear Load (6-Diodes Rectifier)	Load resistor R _{dc}	40 Ω
	Load resistor L _{dc}	30 mH
Shunt Active Power Filter (SAPF)	Interface Resistor R _f	1 Ω
	Interface Inductor L _f	3 mH
	DC side Capacitor C _{dc}	1.8 mF
	References Voltage V _{dc,ref}	650 V

6. Simulation Results and Discussion

The simulation and obtained results are carried out in MATLAB/SIMULINK environment. The initialization data for proposed PSO, AHA, AOA, and MOA algorithms are shown in table 2.

Table 2. Initialization Data for Proposed Optimization Algorithms

Algorithm	Variables Number		Variable Limits		Objective function	Population Number	Max. Iteration Number
			K _p [lower-upper]	K _i [lower-upper]			
PSO	K _p	K _i	50:250	1: 15	THD _i	10	150
AHA							
AOA							
MOA							

6.1. Simulation scenarios

In this section, the gains of the PI-controller are optimized to improve the value of the source current THD. Then, the performance of the controller is evaluated under the static non-linear load connected at the PCC. This evaluation was implemented according to the following scenarios.

- Scenario 1. Without connected SAPF.
- Scenario 2. With connected SAPF without PI-controller tuning.
- Scenario 3. With connected SAPF and PI-controller tuned by PSO.
- Scenario 4. With connected SAPF and PI-controller tuned by AHA.

- Scenario 5. With connected SAPF and PI-controller tuned by AOA.
- Scenario 6. With connected SAPF and PI-controller tuned by MOA.

6.1.1. Scenario 1. Without connected SAPF.

In this case, SAPF is disconnected and the distortion in source current caused by the nonlinear load is obtained by Fast Fourier Transform (FFT) analysis which calculated about 24.2358%. Figure 8 (a) shows the three-phase simulation waveforms for source and load currents. Figure 8 (b) shows FFT harmonic spectrum for the source current.

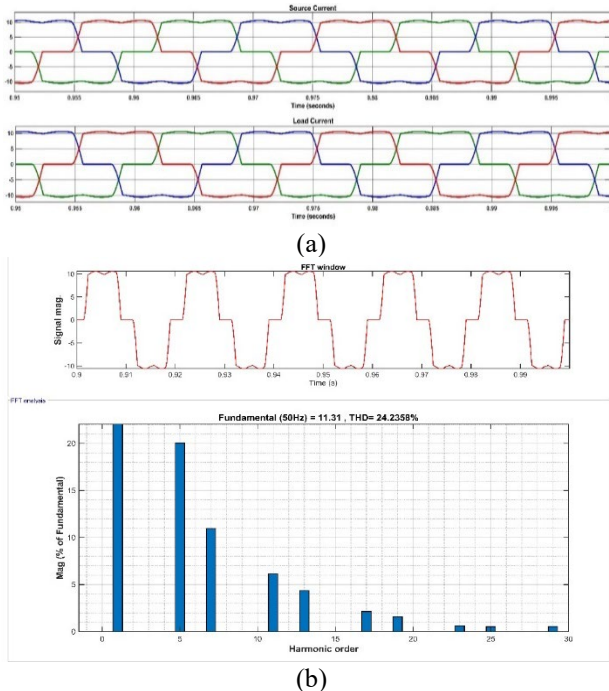


Fig. 8. (a) Simulation waveforms without SAPF, (b) THD; harmonic spectrum

6.1.2. Scenario 2. With connected SAPF without PI-controller tuning.

In this case, SAPF is connected at PCC, the simulation results are taken without tuning of PI-controller gains. The distortion in supply current distortion after SAPF compensation is reduced and becomes 2.229%. The simulation waveforms for source current, load current, and the compensating filter current and harmonic spectrum for the source current are shown respectively in Fig. 9 (a), (b).

6.1.3. Scenario 3. With connected SAPF and PI-controller tuned by PSO.

In this case, the simulation operated with SAPF compensation action, and PI-controller gains are tuned by PSO Algorithm. The obtained results indicate that the THD_i for the source current is reduced to 1.548% when $K_p=50$, and $K_i=14.2285$. Figure. 10 (a) shows waveforms of source current, load current, and the compensating SAPF current. Figure. 10 (b) shows the harmonic spectrum for the source current.

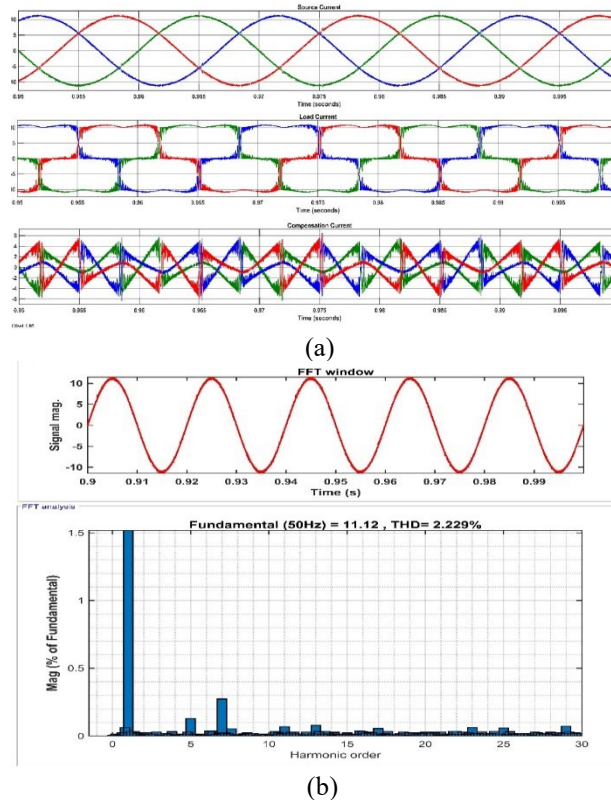


Fig. 9. (a) Simulation waveforms without PI-controller tuning, (b) THD; harmonic spectrum

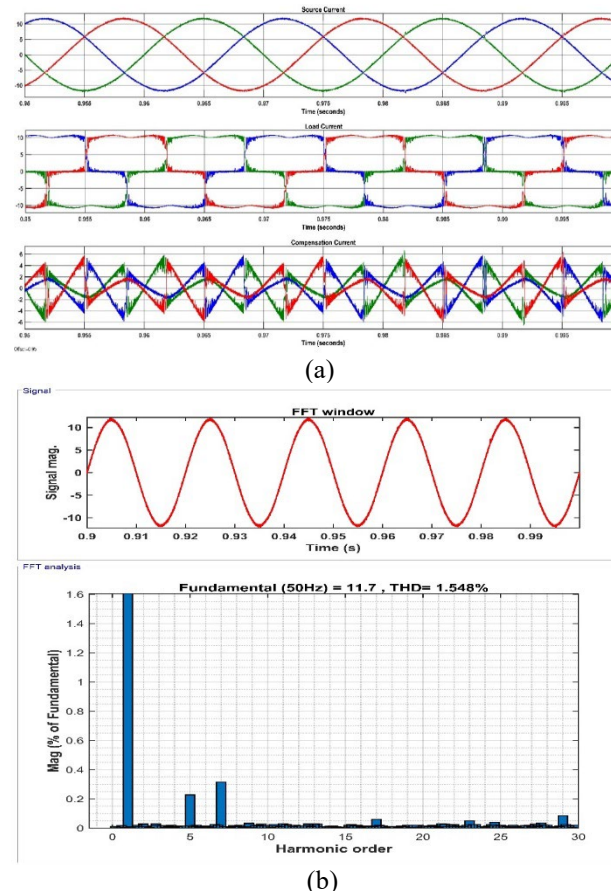


Fig. 10. (a) Simulation waveforms with PI-controller tuned by PSO, (b) THD; harmonic spectrum

6.1.4. Scenario 4. With connected SAPF and PI-controller tuned by AHA.

The obtained results with the AHA algorithm indicate that the THD_i is reduced to 1.545% when K_p =51.3482, and K_i=4.7282. Figure. 11 (a) shows simulation waveforms for all source, load, and compensating currents. Figure. 11 (b) shows the source current THD_i harmonic spectrum.

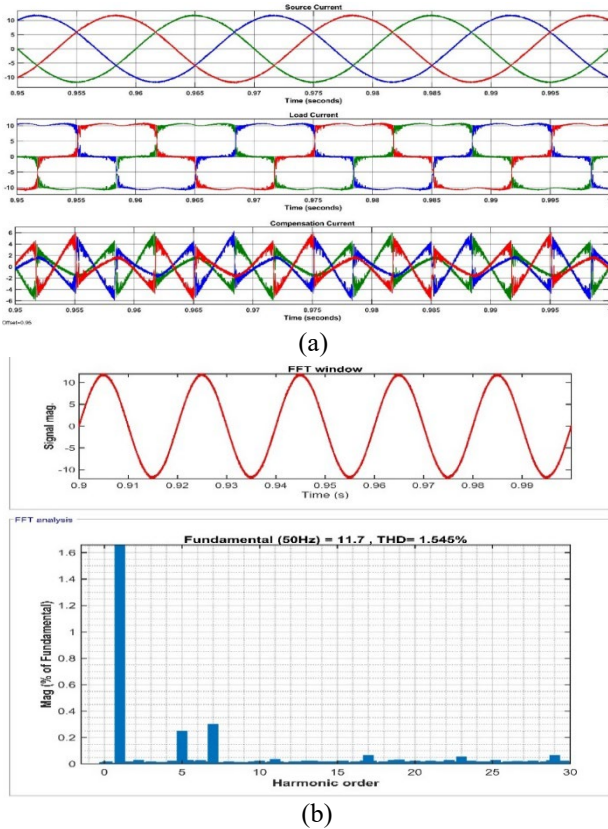


Fig. 11. (a) Simulation waveforms with PI- controller tuned by AHA, (b) THD_i harmonic spectrum

6.1.5. Scenario 5. With connected SAPF and PI-controller tuned by AOA.

Distortion for supply current signal is decreased to 1.539% with K_p =50, and K_i= 4.8194 when tuning PI-controller using the AOA algorithm. The waveforms for all current signals are shown in Fig. 12 (a), and THD_i harmonic spectrum value obtained by FFT is shown in Fig. 12 (b).

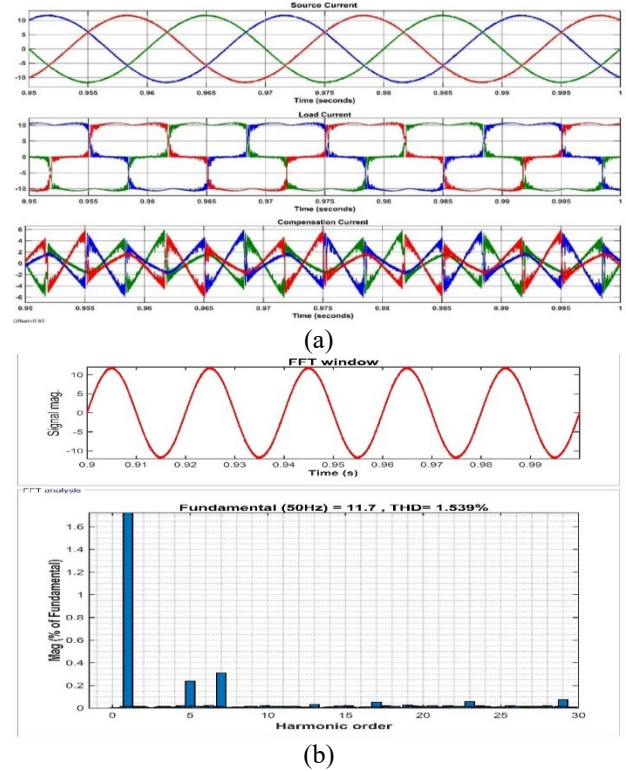


Fig. 12. (a) Simulation waveforms with PI- controller tuned by AOA, (b) THD_i harmonic spectrum

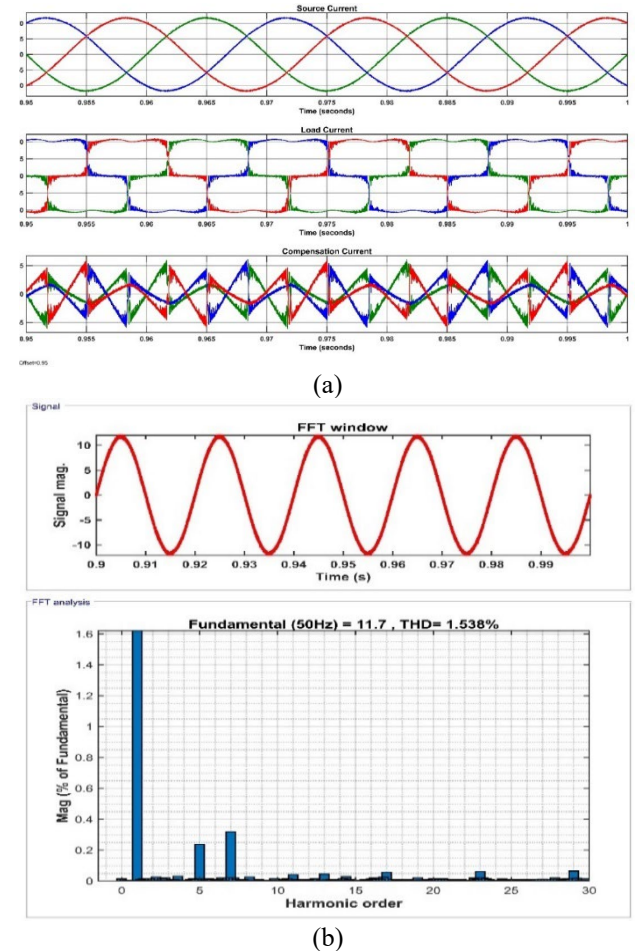


Fig. 13. (a) Simulation waveforms with PI- controller tuned by MOA, (b) THD_i harmonic spectrum

6.1.6. Scenario 6. With connected SAPF and PI-controller tuned by MOA

PI-controller gains are tuned using the MOA algorithm and the best fitness (minimized THD_i) is mitigated to 1.538% at the best solutions K_p = 59.3682, and K_i= 1.3344. Fig. 13 (a) shows source current, load current, and the compensating current waveforms. Fig. 13 (b) shows the THD_i spectrum for the drawn supply current.

6.2. Comparison Between the Optimized Results for all suggested Algorithms

As shown in table 3 and fig.14, the performance of the SAPF is improved clearly with MOA tuning PI-controller and based on the optimized gains the minimization of THD_i objective function is obtained and its best fitness value becomes 1.538% which is the least value compared with values taken from other algorithms, and it converged at 66 iteration which is the fastest algorithm.

Table 3. Control Parameters, THD_i fitness, Convergence iteration results for the proposed Algorithms

Proposed tuning Algorithm	Best of fitness (THD _i)	Best solutions		Convergence iteration
		K _p	K _i	
PI-Controller without tuning	2.229%	1	1	--
PI-Controller tuned by PSO	1.548%	50	14.2285	78
PI-Controller tuned by AHA	1.545%	51.3482	4.7282	84
PI-Controller tuned by AOA	1.539%	50	4.8194	87
PI-Controller tuned by MOA	1.538%	59.3682	1.3344	66

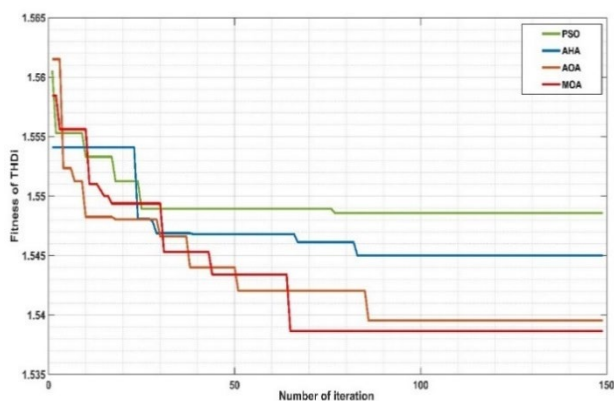


Fig. 14. Fitness function Iterative convergence characteristics for four optimization algorithms

Figure 15 illustrates the speed and accuracy of DC-link voltages for matching the reference value for the suggested algorithms used. It shows that the MOA is the fastest and closest to the reference value with accepted settling time, dc-link voltage overshoot, and steady-state error which attain more enhancement for SAPF controller performance.

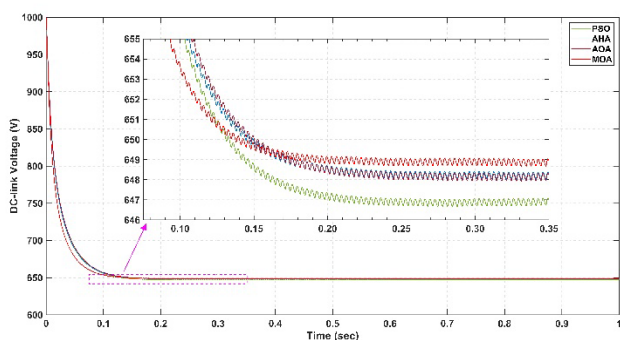


Fig. 15. Response of DC-link voltage values with its reference value for four optimization algorithms

6.3. Evaluation of The Performance of The Optimized Controller Under Variable Load Condition

In this section, the performance of the optimized controller is evaluated under dynamic conditions. In addition to the non-linear load which connected at the PCC, double three-phase RLC loads are connected to the PCC with double three-phase circuit-breakers. Each load has a power capacity equal to one-half of the non-linear load. One of these breakers switches off/on at times 0.2 sec. and 0.4 sec. and the other breaker switches on at a time of 0.4 sec. So, the simulation time is divided into three intervals:

- Interval one of ($0 \leq t \leq 0.2$ sec), and the connected load consists of the non-linear load with a single RLC load.
- Interval two ($0.2 \leq t \leq 0.4$ sec), and the connected load only consists of the non-linear load.
- Interval three ($0.4 \leq t \leq 1$ sec), and the connected load consists of the non-linear load with double RLC loads.

The source current, load current, and compensation current waveforms under variable load conditions are shown in fig. 16 for all intervals.

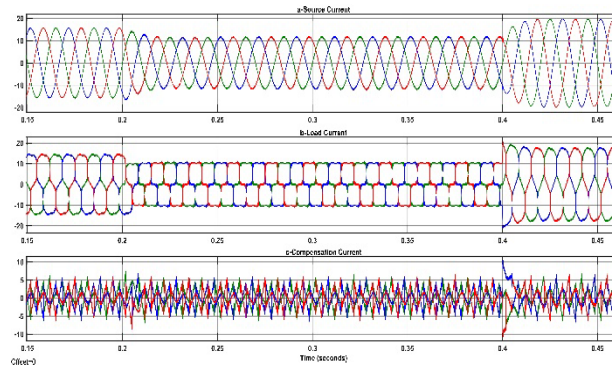


Fig. 16. Simulation waveforms under variable load conditions

Using FFT analysis, the THD of the source current was calculated under variable load conditions to evaluate the performance of the optimized gain controller. Table 4 illustrates the THD of the source current over all intervals. This is obtained using the controller when its gains are tuned by the MOA.

For a better evaluation of the control performance, it is necessary to study the response of the DC-link voltage under dynamic condition, so fig. 17 represent the dynamic response of DC-link voltage values concerning its reference value under variable load condition for all using algorithms. Fig. 17 also shows that MOA is always controlled by the DC-link voltage close to the reference value with minimum steady state error which attains more enhancement for SAPF controller performance.

Table 4. THD_i under variable load condition

Proposed tuning Algorithm	THD _i %		
	0 ≤ t ≤ 0.2	0.2 ≤ t ≤ 0.4	0.4 ≤ t ≤ 1
Without SAPF	17.921	24.236	14.641
PI-Controller without tuning	1.031	2.229	0.473
PI-Controller tuned by PSO	1.022	1.548	0.454
PI-Controller tuned by AHA	1.002	1.545	0.442
PI-Controller tuned by AOA	0.987	1.539	0.421
PI-Controller tuned by MOA	0.829	1.538	0.381

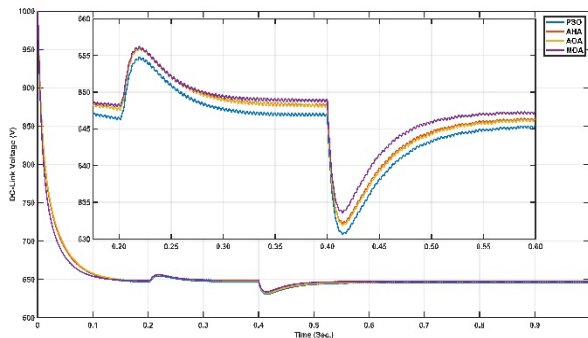


Fig. 17. Response of DC-link voltage values with its reference value under variable load condition

7. Conclusion

In this proposed system including a SAPF controller with dc-link voltage applied a Mayfly Optimization Algorithm (MOA) to optimize the PI-controller gain values and tested with simulation compared to other optimization algorithms, and all optimized results are investigated with the conventional PI-control scheme. The suggested MOA algorithm provides better performance with the least number of iterations compared with the other algorithms. Besides that, the MOA algorithm introduces a better accuracy due to the optimized output parameters for SAPF like THD of the source current, settling time, steady state error of Dc-link voltage, and peak overshoot.

The succeeding conclusions have been ended from the previous study:

1. Effectively compensate for 24.2358%. THD due to current harmonics and reactive power generated by non-linear load and the purposed controller technique mitigates the supply current THD well within acceptable and standard value below 5% and the source current becomes sinusoidal.

2. With all tuning PI-controller optimization methods, all THD values are less than the value obtained without PI-controller tuning, and DC-link capacitor voltage returns its reference value without any deviation against the conventional PI-controller.

3. MOA outperforms a great, most accurate performance, and best correlation dc-link voltage reference voltage compared to other PSO, AHA, and AOA algorithms, and gives a minimum THD value of 1.538 % for the source current.

4. Also, under variable load conditions, MOA gives the best results over all three intervals, where the THD values are 0.829%, 1.538%, and 0.381% respectively. In addition, it gives a great performance in DC-link voltage response under dynamic conditions.

5. Based on all results obtained in this paper, in future works, this proposed efficient controller can be implemented as an interfacing stage between the electric utility and one of the renewable energy sources (RES) such as a photovoltaic (PV) system, wind energy system, also as a stage in the presence of electric vehicles system.

References

- [1] B. Jahnvi, S. B. Karanki, P. Kumar, "Power quality improvement with D-STATCOM using combined PR and Comb filter- Controller", 1st International Conference on Power Electronics and Energy (ICPEE), pp. 1-6, IEEE, 2021.
- [2] IEEE Standard 519-2014, Recommended practice and requirements for harmonic control in electric power systems", The Institute of Electrical and Electronics Engineers, IEEE, 2014.
- [3] R. Kazemzadeh1, E. N. Aghdam, M. Fallah, Y. Hashemi "Performance Scrutiny of Two Control Schemes Based on DSM and HB in Active Power Filter", Journal of Operation and Automation in Power Engineering, Vol. 2, No.2, pp.103-112, Jul 2014.
- [4] H. Özkaya "Parallel Active Filter Design, Control, And Implementation", Master's Thesis, Graduate School of Natural and Applied Sciences of Middle East Technical University, June 2007.
- [5] P. Nammalvar, R. Subburam, U. Ramkumar, M. Padmanaban. "Fuzzy tuned real and reactive power regulation in GC-VSI for PV systems", International Journal of Electronics, pp.1-17, Feb 2022.
- [6] Shahid, "Smart Grid Integration of Renewable Energy Systems," 2018 7th International Conference on Renewable Energy Research and Applications (ICRERA), pp. 944-948, 2018.
- [7] A. M.A. Soliman, T. A. Kandil, M. A. Mehanna, S. K. EL-Sayed, "Mitigation of the Effect of HVDC System on Power System Quality at Distribution Level", International Journal of Engineering and Innovative Technology (IJEIT) Vol.4, No.6, 2014.
- [8] A. M. A. Soliman, S. K. EL-Sayed, M. A. Mehanna, "Assessment of Control Strategies for Conventional and Multi-Functional Inverter Interfacing Power Grid with Renewable Energy Sources (RES)", International Journal of Scientific & Engineering Research Vol. 8, No. 8, August-2017.

- [9] M. Sabarimuthu, N. Senthilnathan, N. Priyadharshini, M. A. Kumar, N. Telagam, S. K. Sree "Comparison of Current Control Methods for a Three Phase Shunt Active Filter", 7th International Conference on Electrical Energy Systems (ICEES), IEEE, 2021.
- [10] S.J. Kumar, R.T. Naayagi, G. Panda, R. D. Patidar, and S. D. Swain. "SAPF Parameter Optimization with the Application of Taguchi SNR Method", *Electronics* 11, no. 3, 348. January 2022.
- [11] Acharya, D. Prasad, S. Choudhury, and N. Nayak. "Optimal Design of Shunt Active Power Filter for Power Quality Improvement and Reactive Power Management Using nm-Predator Prey Based Firefly Algorithm." *International Journal of Renewable Energy Research (IJRER)* Vol.12, No.1, March 2022.
- [12] B. M. Babu, N. U. Kumar, K. S. Kumar, A. Amarendra, B. Bindhu, "SAPF for Power Quality Improvement Based on PODE Optimization Algorithm", *International Journal of Engineering and Advanced Technology (IJEAT)*, Vol.9, No. 3, February 2020.
- [13] V. Habermann Avila and V. Leite, "Control of grid-connected inverter output current: a practical review," 2020 9th International Conference on Renewable Energy Research and Application (ICRERA), pp. 232-235, 2020.
- [14] J. Kennedy, R. Eberhart, "Particle Swarm Optimization", *Proceedings of IEEE international conference on neural networks*, pp 1942-1948, 1995.
- [15] S. Bangia, P. R. Sharama, M. Garg, "Comparison of Artificial Intelligence Techniques for the Enhancement of Power Quality", *International Conference on Power, Energy and Control (ICPEC)*, 2013.
- [16] S. Vadi, F. B. Gurbuz, S. Sagioglu and R. Bayindir, "Optimization of PI Based Buck-Boost Converter by Particle Swarm Optimization Algorithm," 2021 9th International Conference on Smart Grid (icSmartGrid), pp. 295-301, 2021.
- [17] O. Aysenur, and M. R. Tur. "A Short Review on the Optimization Methods Using for Distributed Generation Planning." *International Journal of Smart Grid-ijSmartGrid* 6, no. 3, pp. 54-64. (2022).
- [18] G. S. Rao, B. S. Goud and C. R. Reddy, "Power Quality Improvement using ASO Technique," 2021 9th International Conference on Smart Grid (icSmartGrid), pp. 238-242, 2021.
- [19] K. P, "Design and Implementation of Shunt Active Power Line Conditioner using Novel Control Strategies", *National Institute of Technology, Rourkela, India -769 008*, August 2012.
- [20] J. Afonso, C. Couto, J. Martins "Active Filters with Control Based on the p-q Theory", *IEEE Industrial Electronics Society Newsletter* vol. 47, no 3, pp. 5-10, Sept. 2000.
- [21] H. Akagi, E. H. Watanabe, M. I. Aredes, "Instantaneous power theory and applications to power conditioning", *The Institute of Electrical and Electronics Engineers, John Wiley & Sons, Inc., Hoboken, New Jersey, USA, Second Edition*, 2017.
- [22] N. K. T. Tam, N. V. Nho, H. H. Tai, N. L. H. Bang, "Design And Implementation Of A Dsp-Based Three-Phase Shunt Active Power Filter", *Journal of Engineering Technology and Education, The 2012 International Conference on Green Technology and Sustainable Development (GTSD)*, 2012.
- [23] R. Kazemzadeh1, E. Najafi Aghdam, M. Fallah, Y. Hashemi "Performance Scrutiny of Two Control Schemes Based on DSM and HB in Active Power Filter," *Journal of Operation and Automation in Power Engineering*, Vol. 2, No.2, pp.103-112, Jul 2014.
- [24] N. Zaveri1, A. R. Chudasama, "Simulation Study and Comparative Analysis of Different Control Techniques Used for Three Phase Three Wire Shunt Active Filters", *International Journal of Electronics Engineering*, 1(2), pp. 227-233, 2009.
- [25] R. Storn, k. price, "Differential Evolution - A simple and special heuristic for global optimization over continuous spaces", *J Global Optim* 11:341-359, 1997.
- [26] C. Wang, D. Ping, B. Song, H. Zhang, "Optimization of Multi-Machine Passive Positioning System Based on PSO", *Comp. Digital Eng.*, 49, 487-492, 2021.
- [27] D. E. Goldberg, J.H. Holland, "Genetic Algorithms and Machine Learning", *Mach. Learn.*, 2, 95-99, 1988.
- [28] X.S. Yang, X. He, "Firefly algorithm: Recent advances and applications", *Int. J. Swarm Intell.* 1, 36-50, 2013.
- [29] A. Hu, Z. Deng, H. Yang, Y. Zhang, Y. Gao, D. Zhao, "An Optimal Geometry Configuration Algorithm of Hybrid Semi-Passive Location System Based on Mayfly Optimization Algorithm". *Sensors*, vol. 21, no.22, 7484, 2021.
- [30] K. Shamaei, J. Khalife, Z.M. Kassas, "Exploiting LTE Signals for Navigation: Theory to Implementation", *IEEE Trans. Wireless Commun*, 17, pp. 2173-2189, 2018.
- [31] A. Durmus, R. Kurban, E. Karakose, "A comparison of swarm-based optimization algorithms in linear antenna array synthesis", *Journal of Computational Electronics*, vol.20, no. 4, pp. 1520-1531, Aug 2021.